The Physics of L and H-mode Confinement in JET

V V Parail[1], B Balet, P Bak, J G Cordey, N Deliyanakis, M Erba, R Giannella, D G Muir, M F F Nave, L Porte, E M Springmann, A Taroni, K Thomsen, G Vayakis.

JET Joint Undertaking, Abingdon, Oxfordshire, OX14 3EA, UK.
[1] Permanent Address: Russian Scientific Centre "Kurchatov Institute", Moscow, Russia.

THE PHYSICS OF L AND H-MODE CONFINEMENT IN JET

V.V. Parail[1], B.Balet, P.Bak, J.G. Cordey, N. Deliyanakis, M. Erba, R. Giannella, D.G. Muir, M.F.F. Nave, L. Porte, E.M. Springmann, A. Taroni, K. Thomsen and G. Vayakis.

JET Joint Undertaking, Abingdon, Oxon, OX14 3EA, UK
[1] Permanent address: Russian Scientific Centre "Kurchatov Institute", Moscow, Russia.

ABSTRACT

The results of numerical simulation of JET L, H and VH mode are presented. It is shown that L-H and H-L transitions are accompanied by a fast and large modification of the transport coefficients not only near the plasma edge but across a large fraction of the plasma cross section. Both experiments and numerical simulations show that giant ELMs on JET also have a global character and their penetration length increases with the amplitude of the D signal. Transport coefficients are of the order of the L-mode ones during these ELMs. Analysis shows also that within the experimental accuracy transport coefficients are the same for VH and ELM-free H mode JET discharges. The difference between them is mainly due to impurity radiation, power deposition profile and different in the plasma recycling and related convection.

1. INTRODUCTION

It has been shown[1], that the transport coefficients (electron and ion thermal diffusivities χ_e and χ_i, plasma diffusion coefficient D and perpendicular viscosity μ) in JET drop over a very wide radial region ($0.5 \leq r/a \leq 1$) in a very short time scale ($\Delta\tau \leq 3$ms for χ_e) at the L-H transition. A possible explanation is that plasma turbulence is correlated in radial direction by the plasma toroidicity[2]. Therefore any modification of the anomalous transport coefficients (at L-H and H-L transitions and during ELMs) could propagate across the magnetic field with the group velocity of plasma turbulence (which is much faster than the velocity of heat pulse propagation). Results of transport analysis of JET discharges are presented which support this idea and allow us to develop transport models which can describe the evolution of plasma parameters in L, ELM-free and ELMy H-modes JET plasma.

2. EXPERIMENTAL RESULTS

Fig.1 shows the temporal evolution of the electron temperature at different radii measured by the new 48 channel ECE Heterodyne Radiometer for a typical low density discharge from the new campaign (#31078 with B_t=2.8T, I_p=2.5MA, $\bar{n}_e \cong 1.5\cdot10^{19}m^{-3}$, P_{NBI}=10MW) together with the D_α signal. It is seen that both L-H and H-L transitions are accompanied by an abrupt change of electron transport over a very wide radial region ($0.5 \leq r/a \leq 1$). The direct comparison of experimental evolution of electron temperature with one calculated under the assumption of either local or global modification of χ_e at the time of L-H transition for #31078 is shown in Fig. 2. This confirms our previous conclusion [4] about global modification of electron transport during the transition. To explain the fast response of the electron temperature using a local model for χ_e, one has to take an extremely nonlinear form for

$$\chi_e \sim \frac{|\nabla T_e|^{m+1}}{T_e^{\ m}} \quad \text{with } m \geq 20.$$

A global modification of plasma transport was also found to take place during giant ELMs. In particular it appears that each giant ELM on JET consists of a short (t≤1ms) broadband burst of MHD turbulence (Fig.3) followed by a much longer (t>>10ms) tail of enhanced transport which extends radially from the separatrix inwards for an extent depending on ELM's amplitude (Fig.4). This concept has been supported by recent measurements of density fluctuations during the L-H transition and giant ELMs, measured by a multi-channel, O-mode reflectometer, spanning the frequency range 18-70kHz, corresponding to critical densities in the range $(0.4\text{-}6)\text{x}10^{19}\text{m}^{-3}$. In the next section the result of numerical analysis of the plasma dynamics at the time of the L-H transition, during ELMs and in the ELM-free H and VH modes will be presented. The main objective of such analysis is to reveal the common and distinctive features of the transport in these regimes.

3. PREDICTIVE MODELLING

The evolution of electron and ion temperatures T_e and T_i was simulated while the plasma density, Z_{eff} and the radiated power were imposed from experiment. Power deposition profiles were taken from TRANSP analysis. The following model for electron and ion thermal diffusivities was used:

$$\chi_e = \frac{c^2}{\omega_{pe}^2}\frac{\varepsilon v_{Te}}{qR} + \alpha_e \frac{c|\nabla(nT_e)|}{eBn} aq^2, \ \chi_i = \chi_i^{neo} + \alpha_i \frac{c|\nabla(nT_e)|}{enB} aq^2 \qquad (1)$$

where the first term on right hand side of χ_e reproduces neoalcator scaling, χ_i^{neo} is the ion neoclassical thermal conductivity and the second term on the right hand side of χ_e and χ_i is an empirical Bohm-like coefficient, proposed and used in [3] to reproduce L-mode confinement in JET. This analysis shows that the numerical coefficients α_e and α_i should be chosen $\alpha_i^{\ L} = 3\alpha_e^{\ L} = 9.9 \cdot 10^{-4}$ to fit JET L-mode discharges. We found that the best agreement with old and new JET shots is achieved if we assume that α_e and α_i are reduced from $\alpha_i^{\ L} = 3\alpha_e^{\ L} = 9.9 \cdot 10^{-4}$ in L-mode to $\alpha_i^{\ H} = 3\alpha_e^{\ H} = 0.54 \cdot 10^{-4}$ in H-mode plasmas. New boundary conditions for T_e and T_i were used in our analysis which correspond to an assumption that the longitudinal heat flux in the SOL is proportional to the particle flow: $\chi_{e,i} n\nabla T_{e,i}|_{r=a} = \beta_{e,i} D T_{e,i} \nabla n|_{r=a}$, where $D = \frac{\chi_e \chi_i}{\chi_e + \chi_i}$ and $\beta_e \sim \beta_i \sim 0.3$ are numerical parameters. These boundary conditions allow us to reproduce the formation of the temperature pedestal after the L-H transition (Fig.5) and to explicitly take into account convective losses.

In our analysis we also tried to quantify the difference between local energy transport in JET hot-ion VH mode and the ELM-free H-mode. To illustrate these points we chose the best hot-ion shot #26087 (B_t=2.8T, I_p=3.2 MA and P_{NBI} =14MW) from the previous campaign and two ELM-free H-mode from the current campaign- ##30591 (B_t=2.8T, I_p=2.5 MA and P_{NBI}=15MW) and 30725 (B_t=2.3T, I_p=3MA and P_{NBI}=7MW). The temporal evolution of the total measured plasma energy content and that calculated with our model during the ELM-free H-mode phase for all discharges are shown in Fig.6. They show that within the experimental accuracy we can fit both kind of shots with the same transport coefficients. The main differences between VH and ELM-free H-mode lie not in transport properties but in the impurity radiation (the H-mode accumulates impurities much faster than the VH mode), power deposition profiles (centrally peaked for VH-mode and flat or even hollow for H-mode) and different level of convective losses (the latter is larger for #30591). This conclusion was recently confirmed by TRANSP analysis.

Finally we have used our transport model for numerical simulation of the giant ELMs. The idea was to find the radial and temporal distribution of enhanced transport during giant ELMs and the magnitude of the χ_e and χ_i increase. The analysis shows that giant ELMs can be modelled by assuming that the coefficients α_e and α_i have the following form: $\alpha_{e,i}^{ELM} = \alpha_{e,i}^{L} \exp\left\{ -\frac{(t-t_0)}{\Delta t} + \frac{(r-a)}{\Delta r} \right\}$, where t_0 is the time of the beginning of ELM and Δt- its duration, Δr is the characteristic radial width of ELM. We chose shot #30952 from new campaign as a reference one because it contains ELMs of all sizes (see Fig.3). Our numerical analysis shows that we can reproduce the temporal and radial evolution of electron temperature by assuming that Δr increases as the D_α signal increases (Δr=40cm for ELM at t=51.47s and Δr= for ELM at t= 52.27s).

CONCLUSIONS

New experimental results from JET support the idea of a global character of plasma turbulence. Both transport analysis and predictive modelling show that the plasma transport coefficients (χ_e, χ_i, D and μ) experience very large (more than one order of magnitude) and very rapid reduction at a time of L-H transition not only near plasma edge but far inside plasma volume. The transport properties of ELM-free H-mode and VH mode on JET are very close. The difference between them is mainly due to the impurity radiation (which might be connected with plasma-wall interaction), power deposition profile and the different role of plasma convection. Finally experiment and numerical simulation show that giant ELMs on JET also have a global character and can be modelled as a temporary H-L transition triggered by an MHD event.

ACKNOWLEDGEMENT.

The authors are grateful to J.P. Christiansen, G. Fishpool, T.T.C. Jones, W. Kerner, K. Lawson, P. Lomas, O.P. Pogutse, R. Sartori, B. Schunke, P. Smeulders, P. Thomas and M.G. von Hellermann for fruitful discussions.

REFERENCES.

[1] Cordey, J.G., Muir, D.G., Neudachin, S.V., Parail, V.V., et al., Plasma Physics and Contr. Fusion, **36**, A267, (1994),

[2] Connor, J.W., Hastie, R.J., and Taylor, J.B. Proc. Roy. Soc. London Ser. A 365, 1 (1979),

[3] Taroni, A., Erba, M, Springmann, E., and Tibone, F. accepted for publication in Plasma Physics and Contr. Fusion,

[4] Parail, V.V., Cordey, J.G., Springmann, E. and Taroni, A. accepted for publication in Nuclear Fusion.

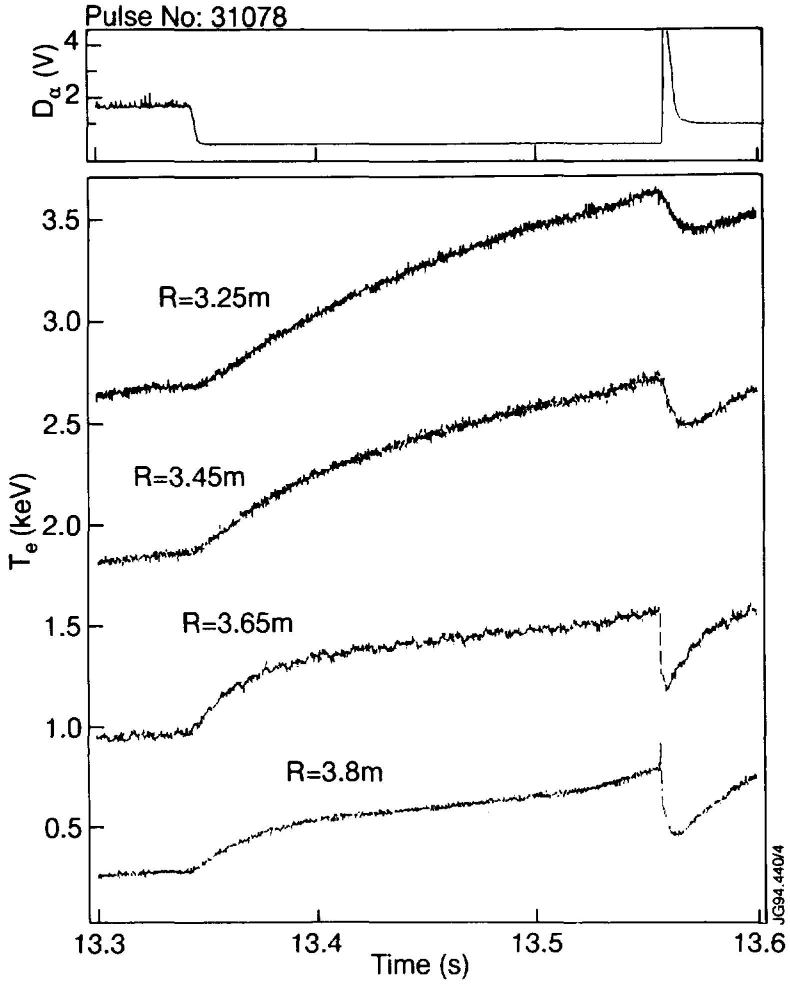

Fig. 1 *Temporal evolution of T_e at different radii and D_α signal for shot #31078.*

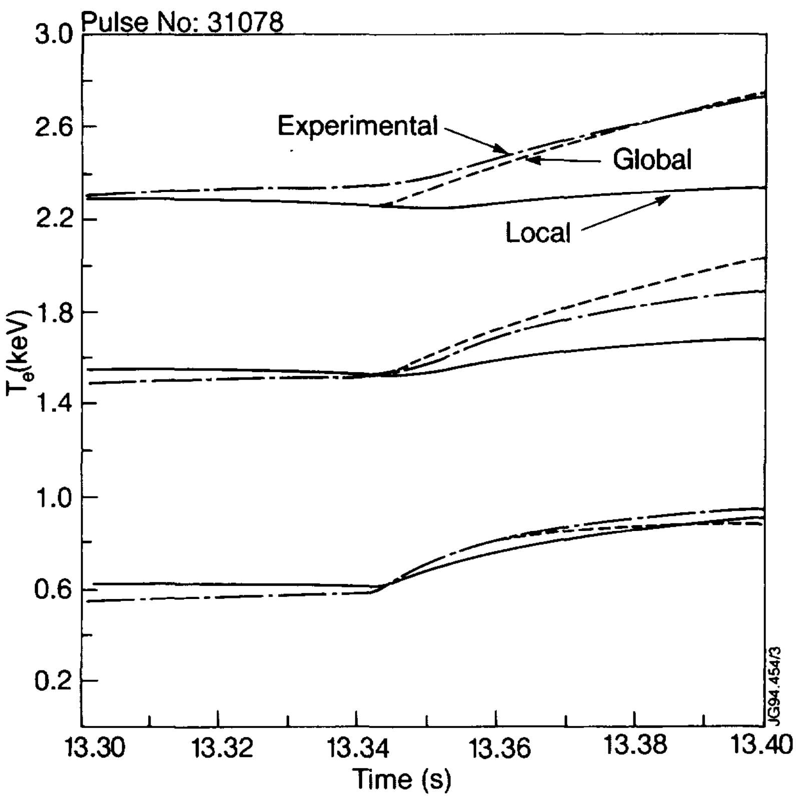

Fig. 2 *Temporal evolution of measured (chain) and calculated T_e under assumption of local (solid) and global (dotted) modification of χ_e.*

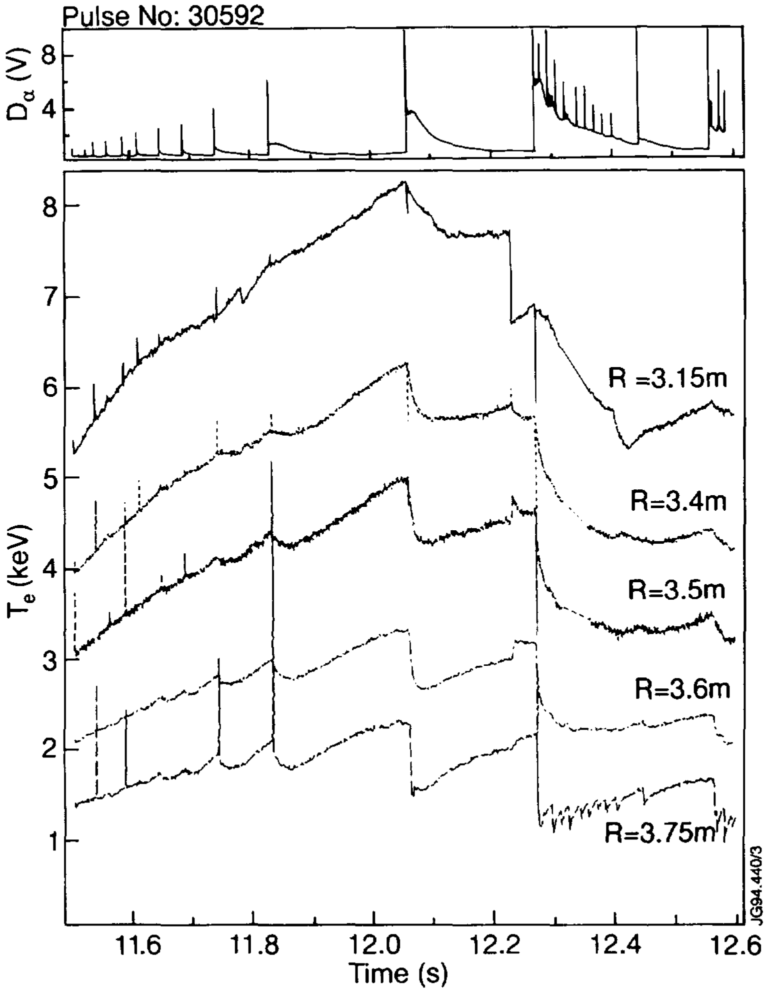

Fig. 3 *Evolution of D_α and fast MHD signals during giant ELM (shot #30929).*

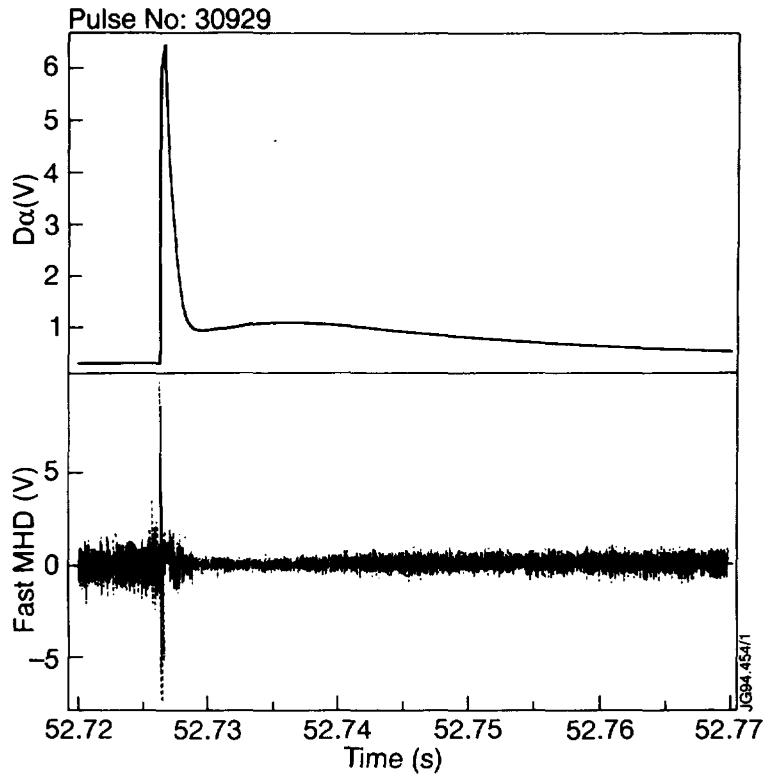

Fig. 4 *Temporal evolution of T_e at different radii and D_α signal for shot #30592.*

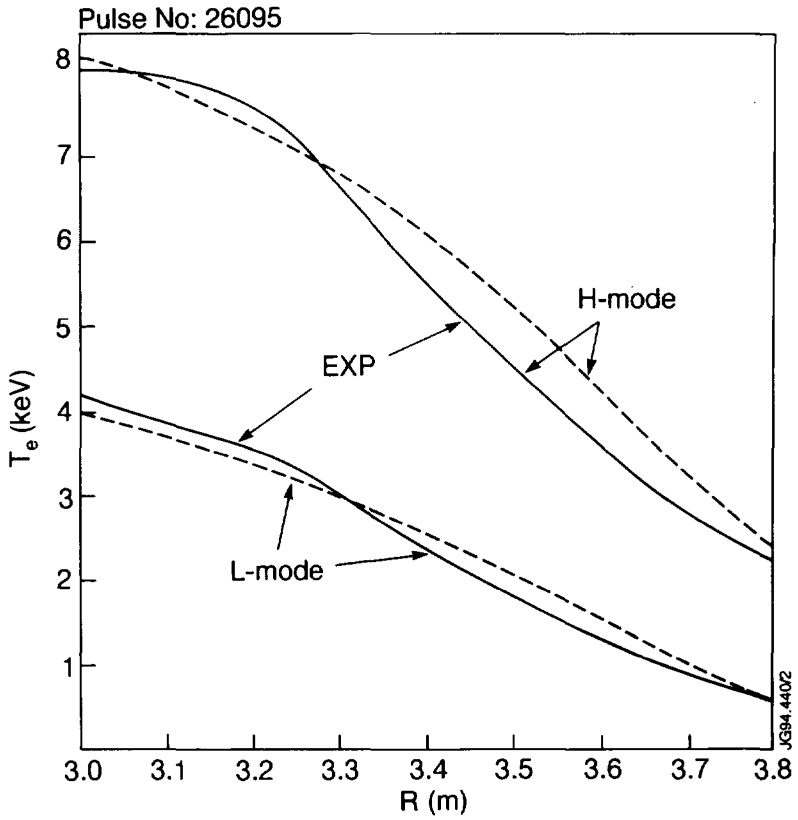

Fig. 5 *Measured and calculated T_e profile for L and H mode phase of shot II 26095.*

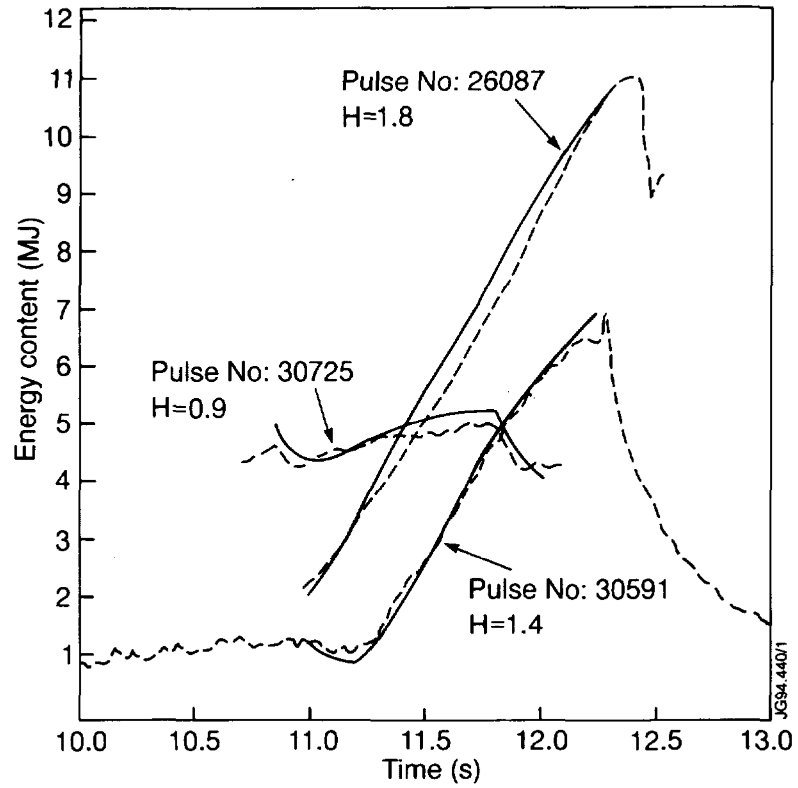

Fig. 6 *Temporal evolution of measured (dashed) and calculated (solid) plasma energy content for ELM free H-modes ($H=\tau_E/\tau_E^{ITER93\text{-}H}$)*